

Continued decay in the cyclotron line energy in Hercules X-1

R. Staubert¹, D. Klochkov¹, V. Vybornov¹, J. Wilms², F.A. Harrison³

¹ Institut für Astronomie und Astrophysik, Universität Tübingen, Sand 1, 72076 Tübingen, Germany

² Dr. Reimis-Sternwarte, Astronomisches Institut der Universität Erlangen-Nürnberg, Sternwartstr. 7, 96049 Bamberg, Germany

³ Cahill Center for Astronomy and Astrophysics, California Institute of Technology, Pasadena, CA 91125, USA

received: 2015 Dec 08, accepted: 2016 March 18

ABSTRACT

The centroid energy E_{cyc} of the cyclotron line in the spectrum of the binary X-ray pulsar Her X-1 has been found to decrease with time on a time scale of a few tens of years - surprisingly short in astrophysical terms. This was found for the pulse phase-averaged line centroid energy using observational data from various X-ray satellites over the time period 1996 to 2012, establishing a reduction of ~ 4 keV. Here we report on the result of a new observation by *NuSTAR* performed in August 2015. The earlier results are confirmed and strengthened with respect to both the dependence of E_{cyc} on flux (it is still present after 2006) and the dependence on time: the long-term decay continued with the same rate, corresponding to a reduction of ~ 5 keV in 20 years.

Key words. magnetic fields, neutron stars, – radiation mechanisms, cyclotron scattering features – accretion, accretion columns – binaries: eclipsing – stars: Her X-1 – X-rays: general – X-rays: stars

1. Introduction

This note is a continuation, an update, and an extension of Staubert et al. (2014), hereafter “Paper 1”, which established the long-term change in the cyclotron line energy in Her X-1. For the introduction to this source, a well-studied accreting X-ray binary pulsar, we therefore refer to Paper 1, except for brief remarks on the cyclotron line. The continuum spectrum (a power law with exponential cutoff) is modified by a line-like feature. This feature, discovered in 1976 in a balloon observation (Trümper et al. 1978), has been re-measured numerous times and is now generally accepted as an absorption feature around 40 keV due to resonant scattering of photons off electrons on quantized energy levels (Landau levels) in the teragauss magnetic field at the polar cap of the neutron star. The feature is therefore also referred to as a *cyclotron resonant scattering feature* (CRSF). The energy spacing between the Landau levels is given by $E_{\text{cyc}} = \hbar e B / (m_e c) = 11.6 \text{ keV } B_{12}$, where $B_{12} = B / 10^{12} \text{ G}$, providing a direct method of measuring the magnetic field strength at the site of the emission of the X-ray spectrum. The observed line energy is subject to gravitational redshift z at the location where the line is formed, such that the magnetic field can be estimated by $B_{12} = (1+z) E_{\text{obs}} / 11.6 \text{ keV}$, with E_{obs} being the observed cyclotron line energy. The discovery of the cyclotron feature in the spectrum of Her X-1 provided the first ever direct measurement of the magnetic field strength of a neutron star, in the sense that no other model assumptions are needed. Originally considered an exception, cyclotron features are now known to be rather common in accreting X-ray pulsars; ~ 25 binary pulsars have now been confirmed as cyclotron line sources (Caballero & Wilms 2012).

The centroid energy of the cyclotron line of Her X-1 has been found to vary systematically with respect to the following variables:

- Variation with phase of the 1.24 s pulsation, with a peak-to-peak amplitude of $\sim 25\%$ (Voges et al. 1982; Vasco et al. 2013);

- Variation with X-ray luminosity, on both long and on short time scales (Staubert et al. 2007; Klochkov et al. 2011);

- Variation with phase of the 35 d precessional period (albeit rather weak) (see Paper 1);

- Variation with time: 1) a rather sharp jump upwards in energy around 1992 (Gruber et al. 2001, Paper 1), and 2) a true decrease in the phase-averaged line energy after 1993 with a magnitude of ~ 5 keV over 20 years (Paper 1; Staubert 2014; Klochkov et al. 2015).

Here we present the results of a new measurement of the line energy by *NuSTAR*, performed in August 2015. The earlier results presented in Paper 1, Staubert (2014), and Klochkov et al. (2015) are confirmed and strengthened with respect to both the dependence of E_{cyc} on flux (it is still present after 2006) and the dependence on time: the long-term decay continued at the same rate.

2. Observations

Her X-1 was observed on August 3–4, 2015, in a campaign coordinated by *NuSTAR* (Harrison et al. 2013) and *INTEGRAL* (Winkler et al. 2003). For this contribution we restrict ourselves to the results of the first 13.5 hr *NuSTAR* observation (ObsIDs 90102002002, MJD 57237.70 – 57238.26) with a total on-source integration time of 27.1 ksec. This is a Main-On observation of 35-day cycle 457 at phase 0.13¹. The mean *NuSTAR* count rate during this time was ~ 43.5 cts/s (5–79 keV). This count rate is very low for Her X-1, but turned out to be quite useful since it extended the dynamical range of observed fluxes (in fact the lowest level at which the cyclotron line energy has ever been measured). We note that for comparing *flux*, we use the maximum *Main-On* flux in units of *RXTE*/ASM-cts/s, as today it is determined through the monitoring observations by *Swift*/BAT. The conversion between these two units is as follows: (2–10 keV ASM-cts/s) = $93.0 \times (15\text{--}50 \text{ keV BAT-cts cm}^{-2} \text{ s}^{-1})$. We determined the re-

Send offprint requests to: staubert@astro.uni-tuebingen.de

¹ For cycle number and phase see Staubert et al. (1983, 2013)

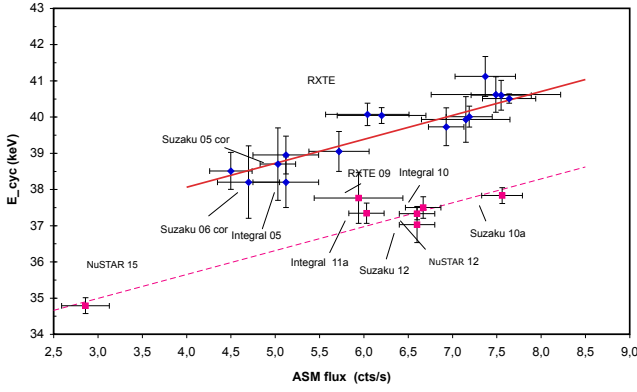


Fig. 1. Positive correlation between the cyclotron line energy and the maximum X-ray flux of the corresponding 35-day cycle. Here, Fig. 1 of Paper 1 is reproduced with the new *NuSTAR* point added: $E_{\text{cyc}}(\text{observed}) = 34.79 \pm 0.22$ keV. The blue diamonds are values observed until 2006, the red dots are after 2006. The solid red line is a linear fit to data until 2006 with the original slope of 0.66 keV/(ASM cts/s), as found by Staubert et al. (2007). The dotted red line is the best fit to the data after 2006 with the slope fixed to the same value. The flux level of the new observation (2.96 ASM-cts/s) is very low, extending the dynamic range of observed fluxes to the low end (missing for the time after 2006). The new value fits well into the general picture.

relationship by using flux measurements of times when both instruments operated simultaneously (see the Appendix). The corresponding *Main-On-flux* for cycle 457 was (2.96 ± 0.28) ASM-cts/s. We have verified that the maximum flux of the *Main-On* is a good measure of the luminosity of the source during the cycle (Vasco et al. 2011).

For this work we have neglected the point measured by *INTEGRAL* in 2012 because of the unexplained high value (see discussion in Paper 1). A re-analysis of these data with the newest calibration, which will be contained in the new analysis software (OSA-11)², to be released later this year, has shown, that this data point indeed needs to be corrected downward. A publication in which calibration issues and the evolution of the various software releases will be discussed in depth is in preparation. We also stress that the inclusion of this point (even with the high value) in no way alters the fit results and the overall conclusions (the statistical weight is simply too low). The results of the other observations from the August 2015 campaign will be presented elsewhere.³

3. Spectral results

The spectral analysis was performed using the standard software as part of HEASoft⁴ (Version 6.16) provided by the *NuSTAR* team. *NuSTAR* employs two focussing X-ray telescopes allowing observations in the 3–79 keV energy range, each with its own CdZnTe pixel detector (Harrison et al. 2013). The calibration of these instruments is described in Madsen et al. (2015). For the Her X-1 analysis, detector events from a region of 120 arcsec radius around the source position were used. A region at the periphery of the field of view with a radius of 80 arcsec was used

² <http://www.isdc.unige.ch/integral/analysis#Software>

³ The data from the simultaneous observations by *NuSTAR* and *INTEGRAL* will allow the respective inter-calibration to be studied again.

⁴ <http://heasarc.nasa.gov/lheasoft>

for background determination (with $1.5 \cdot 10^{-3}$ of the Her X-1 flux, which is negligible). Both telescopes/detectors were used to generate spectra in the 5–79 keV range. When combining these data for a common spectrum, a normalization factor was a free parameter.

For the spectral model we chose the *highecut*⁵ model, which is based on a power law continuum with exponential cut-off; the CRSF is modeled by a multiplicative absorption line with a Gaussian optical depth profile. In order to smooth the jump in the derivative of the *highecut* function at E_{cut} , a multiplicative Gaussian was used, as in Coburn et al. (2002). The spectral fit is good (reduced $\chi^2 = 1.14$ for 1777 degrees of freedom (dof)), yielding parameters that are very consistent with those found previously. The observed centroid energy of the CRSF is $E_{\text{cyc}} = 34.79 \pm 0.22$ keV. Throughout this work uncertainties quoted are at the 1σ (68%) level.

4. Variation of E_{cyc} with luminosity

After the first observations of Her X-1 by *RXTE* in 1996 and 1997 which yielded E_{cyc} values slightly lower than those of *CGRO/BATSE* and *Beppo/SAX* a few years earlier, we had suspected that there might be a slow decay of E_{cyc} with time. This motivated repeated and successful observing proposals over the following two decades. In a series of *RXTE* observations until 2005, the apparent decrease seemed to continue until this date. While working with a uniform set of *RXTE* data between 1996 and 2005 trying to establish this decrease, we instead discovered that there was a dependence of E_{cyc} on X-ray flux (Staubert et al. 2007). This degraded the suspected decrease with time significantly, such that it was neglected at this time. The correlation found between E_{cyc} and flux (luminosity) was positive, i.e., the cyclotron line energy E_{cyc} increases with increasing X-ray luminosity L_X . Her X-1 was thus the first source that showed the opposite behavior to those high luminosity transient sources in which a negative correlation had already been seen in 1995 (Mihara 1995). Today we know more confirmed sources with a positive correlation than with the negative one, see Sect. 7.

Figure 1 reproduces the correlation graph of Paper 1 (Fig. 1) with the new data point added (“*NuSTAR* 15”): the observed pulse phase averaged CRSF centroid energy is $E_{\text{cyc}} = 34.79 \pm 0.22$ keV. As noted in Paper 1, the values after 2006 are significantly lower than those before, which already clearly signals a decrease in the cyclotron line energy with time. In the earlier plot of 2014 the flux dependence for data after 2006 was less obvious. The new data point nicely confirms our previous assumption that the same flux dependence prevailed after 2006 (dotted red line in Fig. 1 is a fit through the data after 2006 with the same slope as the solid red line).

5. Variation of E_{cyc} with time: the long-term decay

The long-term decay of the pulse phase-averaged cyclotron line energy E_{cyc} was finally established by Staubert et al. (2014) (Paper 1) using data from different observatories taken between 1996 and 2012. A linear reduction in E_{cyc} of ~ 5 keV over a time frame of 20 yrs was measured with high significance (~ 18 standard deviations).

Here, we add the latest data point taken by *NuSTAR* in August 2015. First, we consider the time evolution of the flux-normalized E_{cyc} for two different time periods: 1996 – 2006 and 2006 – 2015 (separated at MJD ~ 54000). The normalization to the reference flux of 6.8 ASM-cts/s was done us-

⁵ <http://heasarc.nasa.gov/xanadu/xspec/manual/>

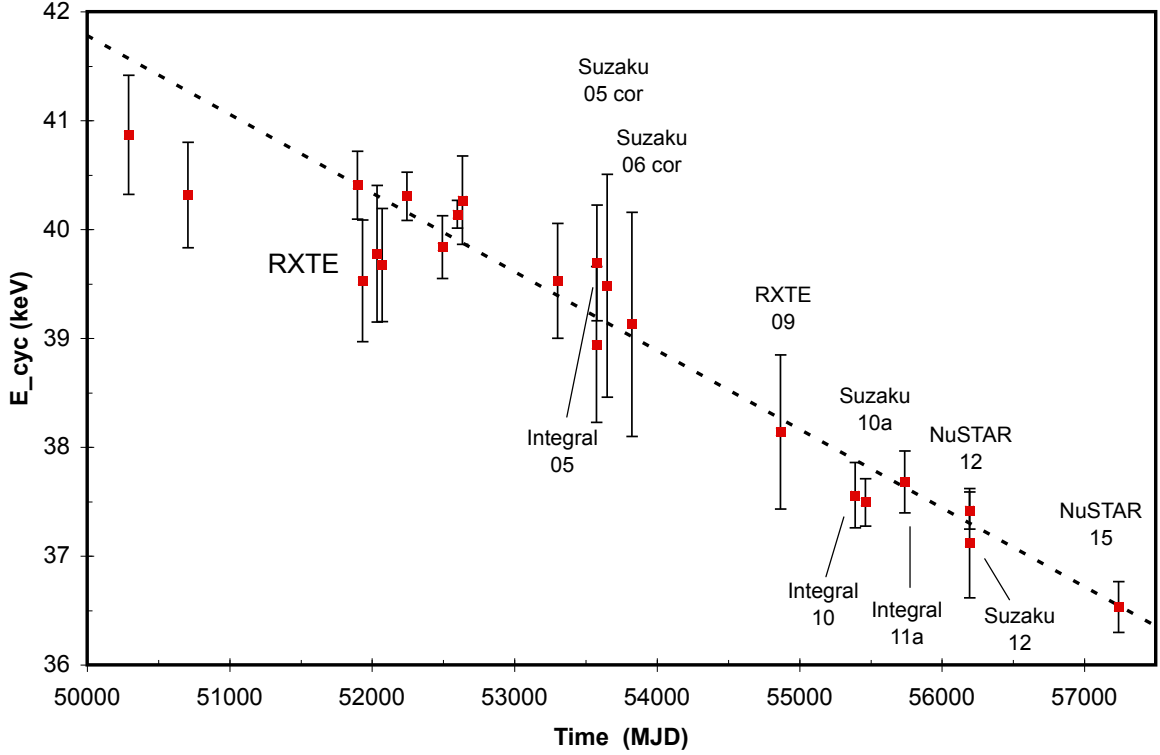


Fig. 2. Her X-1 pulse phase averaged cyclotron line energies E_{cyc} normalized to a reference ASM count rate of 6.8 cts/s using a flux dependence of 0.44 keV/ASM-cts/s. The new flux-normalized *NuSTAR* 2015 value is 36.49 ± 0.24 keV. The best fit dashed line defines a linear decline of E_{cyc} with time with a slope of -7.23×10^{-4} keVd $^{-1}$.

ing a slope of 0.44 keV per ASM-cts/s, which is the best fit slope from the simultaneous flux- and time-dependence of the previous data set. The slopes for those two time periods are $(-3.2 \pm 0.7) \times 10^{-4}$ keV/day and $(-7.0 \pm 0.4) \times 10^{-4}$ keV/day, respectively, constituting a significant steepening in the later period.

We then repeat the simultaneous fit with two variables (the dependence on X-ray flux and the dependence on time) as in Paper 1, with the *NuSTAR* 2015 point added, such that the complete data set of 1996 – 2015 is used.⁶ In order to separate the two variables, the following function was used:

$$E_{\text{cyc}}(\text{calc}) = E_0 + a \cdot (F - F_0) + b \cdot (T - T_0) \quad (1)$$

with F being the X-ray flux (the maximum flux of the respective 35d cycle) in units of ASM-cts/s, as observed by *RXTE*/ASM (and/or *Swift*/BAT), with $F_0 = 6.80$ ASM-cts/s, and T being time in MJD with $T_0 = 53500$. The bi-linear fit is a good description of the complete 1996–2015 data set. The fit parameters are given in Table 1. A comparison of the fit parameters with those of fit No. 4 in Table 4 of Paper 1, shows that all parameters are unchanged (only the uncertainty of parameter “a” describing the flux dependence is slightly smaller now).

Equation (1) constitutes a plane in 3D space defined by the three quantities ASM-flux, time, and E_{cyc} . In principle, the situation could be displayed by a 3D plot. Such a plot (also in-

Table 1. Parameters of the bi-linear fit with Equation (1) to E_{cyc} values observed between 1996 and 2015 (excluding *INTEGRAL* 12). The reference flux is $F_0 = 6.8$ (ASM-cts/s) and the reference time is $T_0 = \text{MJD } 53500$.

E_0 [keV]	a [keV/ASM-cts/s]	b [10^{-4} keV/d]	χ^2	dof
39.25 ± 0.07	0.44 ± 0.06	-7.23 ± 0.39	20.4	19

cluding the data points), however, is not easy to read in practice. We therefore show two corresponding 2D plots that make use of normalized values.

1) We normalized the observed E_{cyc} values to the reference flux of 6.8 (ASM-cts/s) using the flux dependence found in the simultaneous fit and plotted it against time. Figure 2 shows the remaining linear time dependence of E_{cyc} , demonstrating the long-term decay of E_{cyc} with a slope of $(-7.23 \pm 0.39) \times 10^{-4}$ keV/day (or -0.26 ± 0.014 keV/yr). The dashed line is the linear best fit. The new data point (“*NuSTAR* 15”) is very consistent with the earlier data.

2) We normalize the observed E_{cyc} values to the reference time $T_0 = \text{MJD } 53500$ using the time dependence found in the simultaneous fit and plotted against flux. Figure 3 shows the remaining linear flux dependence of E_{cyc} . The slope is

⁶ All points in this data set are from observations taken during the *Main-On* of Her X-1 at 35 d phases less than 0.2.

$0.44 \pm 0.06 \text{ keV}/(\text{ASM-cts/s})$, which is the same as in Paper 1, but slightly lower than the value first found in the discovery paper of Staubert et al. (2007), where only data until 2005 and no time dependence were considered.

After including the 2015 data point of *NuSTAR*, the fact noted in Paper 1 that the fit is slightly better when an additional quadratic term ($c(T - T_0)^2$) in the time dependence is introduced, continues to be valid: $E_0 = (39.41 \pm 0.11) \text{ keV}$, $a = (0.38 \pm 0.07) \text{ keV}/\text{ASM-cts/s}$, $b = -(6.68 \pm 0.48) 10^{-4} \text{ keV/d}$, and $c = -(5.3 \pm 2.8) 10^{-8} \text{ keV/d}^2$, with $\chi^2 = 16.7$ for 18 degrees of freedom. The improvement in χ^2 with respect to the purely linear fit is, however, marginal; an F-test gives a probability of 6.1% for the improvement in χ^2 being by chance when introducing the quadratic term.

If we determine the decay rate of E_{cyc} in the very recent time frame, using only the two values measured by *NuSTAR* in 2012 and 2015, we find $(-8.5 \pm 0.3) \times 10^{-4} \text{ keV/day}$. We note that, owing to the very accurate measurements by *NuSTAR*, the uncertainty is quite small (similar to that of the fit to the complete data).

We also refer to the independent analysis of spectral measurements by *Swift*/BAT, which confirms the decay of E_{cyc} over the time frame 2005–2014 (Klochkov et al. 2015). In this work each data point is an average over several 35-day cycles, neglecting (in a sense averaging over) the flux dependence of the cyclotron line energy. Adding these points (which generally have larger uncertainties) to the previous data set, we find that they closely match the earlier picture and the parameters of the linear fit (simultaneous in flux and time) are not changed. However, owing to the wider spread of the BAT data, the reduced χ^2 is significantly increased (from ~ 1 to beyond 3).

With reference to the Appendix and Fig. A.2 we need to modify the statement made in Paper 1 that the mean maximum X-ray flux (when averaged over several 35d cycles) is constant. A new analysis has now found that the data of the last 20 yrs formally define a slight flux reduction of $0.95 \pm 0.07 \text{ ASM-cts/s}$. We note, however, that the scattering of the individual maximum flux measurements is on the same order of magnitude, the observed variation over several 35d cycles can even exceed 100% (a factor of two).

6. Summary of observational results

The current situation regarding the variation of the phase-averaged cyclotron line energy with luminosity and with time is the following:

1. The latest measurement of E_{cyc} confirms that the long-term decay of the cyclotron line energy continues as before, with a rate of $-(0.260 \pm 0.014) \text{ keV/yr}$ (see Fig. 2). An independent confirmation of the decay is provided by *Swift*/BAT observations for the time interval 2005–2014 (Klochkov et al. 2015). This work provides an idea about the evolution of the originally measured (not flux normalized) E_{cyc} values, in a similar way to that in Fig. 4 of Paper 1.
2. The dependency of E_{cyc} on flux (or luminosity) as detected by Staubert et al. (2007) is still valid after 2006 (see Fig. 1 and Fig. 3). In the combined flux- and time-dependent analysis of the data available until 2012 (Paper 1) this was an assumption that has now been nicely confirmed (with the help of the accidentally low flux during the last observation - even though regrettable from the statistics point of view).

We would like to add another remark related to the unusually low flux level that we encountered during the 2015 *NuSTAR* observation. We have since realized that Her X-1 was on

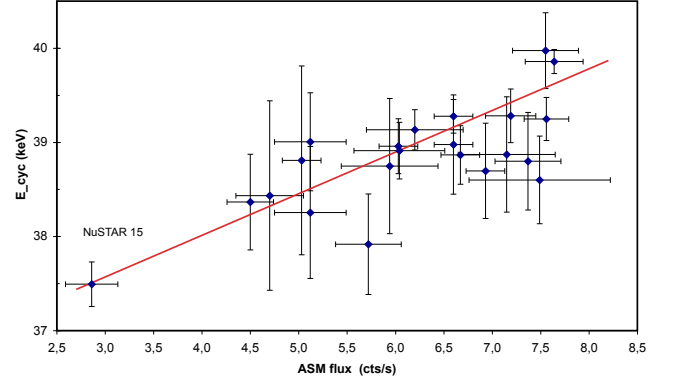


Fig. 3. Her X-1 pulse-phase-averaged cyclotron line energies E_{cyc} normalized to the reference time MJD 53500 using a time dependence of $-7.22 \times 10^{-4} \text{ keVd}^{-1}$. The new time-normalized *NuSTAR* 2015 value is $37.49 \pm 0.24 \text{ keV}$. The solid line defines the linear best fit for the flux dependence of E_{cyc} with a slope of $0.44 \text{ keV}/(\text{ASM-cts/s})$.

its way to a new *anomalous low* that was reached around MJD 57340. Such lows happen irregularly on a time scale of ~ 5 yrs or ~ 10 yrs. It is a known feature that the flux fades gradually when going into such a low (Coburn et al. 2000). We would like to point out that the perfect correlation between flux and E_{cyc} (Fig. 3) indicates a true reduction of luminosity (accretion rate) in the source, and not a reduction in observable flux by a progressing shading of the X-ray emitting region by the accretion disk. This view is further supported by the fact that the entrance into a new *anomalous low* coincides with a strong spin-down⁷ (owing to a reduced mass accretion rate).

3. It is conceivable that the decay of E_{cyc} is actually accelerating with time. Even though the combined fit with a quadratic term in the time dependence yields only marginal evidence for a true (negative) quadratic term, a change in the decay rate is supported by the following two facts. First, using flux-normalized values, we find that the decay of E_{cyc} is stronger during the more recent period 2006–2015 than during 1996–2006 (see Section 5). This steepening is highly significant, and is in line with the remark already made in Paper 1 that in the earlier period the flux dependence is the dominant effect, while in the later period it is the time dependence. Second, using the two observations by *NuSTAR* in 2012 and 2015 alone, a decay rate of $(-8.5 \pm 0.3) \times 10^{-4} \text{ keV/day}$ is found, which is slightly steeper than the slope for the overall decay from 1996–2015 (see Table 1).
4. The slight flux reduction of $\sim 15\%$ between 1996 and 2016 (see Fig. A.2 in the Appendix) corresponds to a reduction in E_{cyc} by $\sim 0.4 \text{ keV}$, when the found flux dependence of $-0.44 \text{ keV}/(\text{ASM-cts/s})$ (see Table 1) is applied. We emphasize that this in no way interferes with the reduction of E_{cyc} with time (by $\sim 5 \text{ keV}$ over 20 yrs), since the long-term flux variation is also taken into account when the two-variable fit (Eq. 1) is applied.

⁷ The Gamma Ray Burst Monitor (GBM) on *Fermi* provides pulse frequencies: <http://gammaray.msfc.nasa.gov/gbm/science/pulsars.html>

7. Discussion

How common are the two dependencies of E_{cyc} - on luminosity and on time - among binary X-ray pulsars? With regard to the dependence on luminosity, the negative correlation (a decrease in E_{cyc} with increasing L_X), was actually discovered first: in high luminosity transient sources from observations by *Ginga* (Mihara 1995). However, of the three sources originally quoted (V 0332+53, 4U 0115+63, and Cep X-4) only one, V 0332+53, can today be considered a secure source.⁸ In Cep X-4 the effect was never confirmed, and in 4U 0115+63, although apparently re-measured (Tsygankov et al. 2006; Nakajima et al. 2006; Tsygankov et al. 2007; Klochkov et al. 2011), Müller et al. (2013) have shown that the anti-correlations are most likely an artifact introduced by the way the continuum was modeled (see also Iyer et al. (2015)).

To the contrary, the positive correlation was only discovered in 2007 by Staubert et al. (2007) in Her X-1, a persistent medium luminosity source. Since then four more sources (all at moderate to low luminosities) have been found with E_{cyc} increasing with increasing luminosity: GX 304-1 (Yamamoto et al. 2011; Klochkov et al. 2012), Vela X-1 (Fürst et al. 2014), A 0535+26 (Klochkov et al. 2011; Sartore et al. 2015) and Cep X-4 (Fürst et al. 2015). As noted above, Cep X-4 is among those sources that were originally considered to show a negative correlation (Mihara 1995), even though the evidence for this source was not very strong and it was never confirmed. It would, however, be quite interesting to find both behaviors (positive and negative correlation) in the same source at very different luminosities. The positive E_{cyc}/L_X correlation might well be a general property of binary X-ray pulsars at low to medium luminosities.

With regard to the long-term change of the cyclotron line energy, Her X-1 is the first and still the only object, for which this phenomenon has been securely established.⁹

For the physical interpretation of the observed phenomena, E_{cyc}/L_X correlation and the long-term change of E_{cyc} , we refer to the discussions in Paper 1 and Staubert (2014). Here we re-iterate only the following general ideas.

We assume that we can distinguish between two accretion regimes: $L_X > L_{\text{crit}}$ (super-critical) and $L_X < L_{\text{crit}}$ (sub-critical). The early explanation for the decrease of E_{cyc} with increasing L_X at super-critical accretion is still popular: based on Basko & Sunyaev (1976), who had shown that the height of the radiative shock above the neutron star surface should grow linearly with increasing accretion rate, Burnard et al. (1991) noted that this means a reduction in field strength and therefore in E_{cyc} . For the positive E_{cyc}/L_X correlation (first seen in Her X-1), Staubert et al. (2007) had proposed that at sub-critical accretion the stopping mechanism of the accreted material is not photon pressure, but is due instead to Coulomb interactions (Nelson et al. 1993), which should lead to the opposite behavior (see also Becker et al. 2012). An alternative explanation, not connected to the height of line emitting region, is to assume changes in the B-field configuration (originally assumed to be a dipole field), suffering distortions due to loading with a variable amount of accreted material (Mukherjee & Bhattacharya 2012). Recently, a new idea has been put forward by Mushtukov et al. (2015), suggesting that a variation in accretion rate should lead to a variation in the velocity distribution of the infalling material in which the cyclotron line is assumed to be generated, such that

a variable Doppler effect is responsible for a shift in the observed line energy.

Regarding the long-term change of the cyclotron line energy, we repeat here our earlier suggestion (Staubert 2014) that a slight imbalance between the rate of accretion and the rate of “losing” material at the bottom of the accretion mound, either by incorporation into the neutron star crust or leaking of material to larger areas of the neutron star surface (Mukherjee et al. 2013, 2014), can lead to a change in the mass loading and consequently in the structure of the accretion mound (height or B-field configuration).

Acknowledgements. The motivation for this paper are new observational data taken by the NASA satellite *NuSTAR*. We would like to acknowledge the dedication of all the people who have contributed to the great success of this mission, here especially Karl Forster for his effort with respect to the non-standard scheduling of the observations. Further important data were provided by the equally successful missions *RXTE* and *Swift* of NASA and *INTEGRAL* of ESA. This work was supported by the Deutsche Forschungsgemeinschaft (DFG) through joint grants KL 2734/2-1 and WI 1860/11-1. We thank the anonymous referee for useful comments and suggestions.

References

- Barthelmy, S. D., Barbier, L. M., Cummings, J. R., et al. 2005, *Space Science Reviews*, 120, 143
- Basko, M. M. & Sunyaev, R. A. 1976, *MNRAS*, 175, 395
- Becker, P. A., Klochkov, D., Schönherr, G., et al. 2012, *A&A*, 544, A123
- Burnard, D. J., Arons, J., & Klein, R. I. 1991, *ApJ*, 367, 575
- Caballero, I. & Wilms, J. 2012, *Mem. Soc. Astron. Italiana*, 83, 230
- Coburn, W., Heindl, W. A., Rothschild, R. E., et al. 2002, *ApJ*, 580, 394
- Coburn, W., Heindl, W. A., Wilms, J., et al. 2000, *ApJ*, 543, 351
- Fürst, F., Pottschmidt, K., Miyasaka, H., et al. 2015, *ApJ*, 806, L24
- Fürst, F., Pottschmidt, K., Wilms, J., et al. 2014, *ApJ*, 780, 133
- Gruber, D. E., Heindl, W. A., Rothschild, R. E., et al. 2001, *ApJ*, 562, 499
- Harrison, F. A., Craig, W. W., Christensen, F. E., et al. 2013, *ApJ*, 770, 103
- Hemphill, P. B., Rothschild, R. E., Markowitz, A., et al. 2014, *ApJ*, 792, 14
- Iyer, N., Mukherjee, D., Dewangan, G. C., Bhattacharya, D., & Seetha, S. 2015, *MNRAS*, 454, 741
- Klochkov, D., Doroshenko, V., Santangelo, A., et al. 2012, *A&A*, 542, L28
- Klochkov, D., Staubert, R., Postnov, K., et al. 2015, *A&A*, 578, A88
- Klochkov, D., Staubert, R., Santangelo, A., Rothschild, R. E., & Ferrigno, C. 2011, *A&A*, 532, A126
- Klochkov, D. K., Shakura, N. I., Postnov, K. A., et al. 2006, *Astronomy Letters*, 32, 804
- Levine, A. M., Bradt, H., Cui, W., et al. 1996, *ApJ*, 469, L33
- Madsen, K. K., Harrison, F. A., Markwardt, C. B., et al. 2015, *ApJS*, 220, 8
- Mihara, T. 1995, PhD thesis, Univ. of Tokyo
- Mukherjee, D. & Bhattacharya, D. 2012, *MNRAS*, 420, 720
- Mukherjee, D., Bhattacharya, D., & Mignone, A. 2013, *MNRAS*, 435, 718
- Mukherjee, D., Bhattacharya, D., & Mignone, A. 2014, in *European Physical Journal Web of Conferences*, Vol. 64, *European Physical Journal Web of Conferences*, 2004
- Müller, S., Ferrigno, C., Kühnel, M., et al. 2013, *A&A*, 551, A6
- Mushtukov, A. A., Tsygankov, S. S., Serber, A. V., Suleimanov, V. F., & Poutanen, J. 2015, *MNRAS*, 454, 2714
- Nakajima, M., Mihara, T., Makishima, K., & Niko, H. 2006, *ApJ*, 646, 1125
- Nelson, R. W., Salpeter, E. E., & Wasserman, I. 1993, *ApJ*, 418, 874
- Sartore, N., Jourdain, E., & Roques, J. P. 2015, *ApJ*, 806, 193
- Staubert, R. 2014, in *PoS(INTEGRAL2014)024*
- Staubert, R., Bezler, M., & Kendziorra, E. 1983, *A&A*, 117, 215
- Staubert, R., Klochkov, D., Postnov, K., et al. 2009, *A&A*, 494, 1025
- Staubert, R., Klochkov, D., Vasco, D., et al. 2013, *A&A*, 550, A110
- Staubert, R., Klochkov, D., Wilms, J., et al. 2014, *A&A*, 572, A119
- Staubert, R., Shakura, N. I., Postnov, K., et al. 2007, *A&A*, 465, L25
- Tananbaum, H., Gursky, H., Kellogg, E. M., et al. 1972, *ApJ*, 174, L143
- Trümper, J., Pietsch, W., Reppin, C., et al. 1978, *ApJ*, 219, L105
- Tsygankov, S. S., Lutovinov, A. A., Churazov, E. M., & Sunyaev, R. A. 2006, *MNRAS*, 371, 19
- , 2007, *Astronomy Letters*, 33, 368
- Vasco, D., Klochkov, D., & Staubert, R. 2011, *A&A*, 532, A99
- Vasco, D., Staubert, R., Klochkov, D., et al. 2013, *A&A*, 550, A111
- Voges, W., Pietsch, W., Reppin, C., et al. 1982, *ApJ*, 263, 803
- Winkler, C., Courvoisier, T. J.-L., Di Cocco, G., et al. 2003, *A&A*, 411, L1
- Yamamoto, T., Sugizaki, M., Mihara, T., et al. 2011, *PASJ*, 63, 751

⁸ http://users.ph.tum.de/ga24wax/2015_W6_slides/Staubert_Talk.pdf

⁹ There are indications, though still fairly weak, for the opposite behavior in 4U 1538–522 (Hemphill et al. 2014)

Appendix A: Determination of X-ray flux and ASM / BAT intercalibration

Here we provide technical details on the procedures used to determine the X-ray flux as well as the intercalibration between *RXTE*/ASM and *Swift*/BAT. Since the start of the operation of the *All Sky Monitor* (ASM) (Levine et al. 1996) on board the NASA satellite *RXTE* in 1996, a high quality continuous monitoring of sufficiently strong X-ray sources has been underway. ASM provides average count rates in the 2–10 keV range (in units of cts/s) for 90 sec long “dwell”s and for one day¹⁰. The operation of ASM ended in early 2010. Since early 2005 the *Burst Alert Telescope* (BAT) (Barthelmy et al. 2005) on board the NASA satellite *Swift* monitors X-ray sources (in addition to detecting gamma-ray bursts). The BAT average count rates are given for the 15–50 keV range in units of cts/(cm² s), both per satellite orbit and per day¹¹. Between 2005 and 2010 both monitors operated simultaneously, allowing an inter-calibration of the two instruments to be established.

A.1. Determination of X-ray flux

As stated in the main text, we take the maximum flux encountered in each *Main-On* as a measure of the local luminosity of this 35d cycle. How is this flux determined? Since the discovery of Her X-1 as an accreting binary X-ray pulsar by *UHURU* in 1972 (Tananbaum et al. 1972), it has been known that the flux varies strongly on three different time scales (in addition to the 1.237 s pulsation): the ~35 d on-off period, the 1.70 d binary eclipses (of ~6 hours duration) and the 1.62 d period with similarly long “dips”. For details on these modulations and the underlying physics, see e.g., Klochkov et al. (2006) and Staubert et al. (2013). Fig. A.1 (upper panel) shows the Her X-1 light curve of the *Main-On* of 35d cycle 462, as measured (in orbital averages) by *Swift*/BAT. All three types of flux modulations are apparent. In order to find a measure of the true intrinsic luminosity (accretion rate), the observed light curves were *cleaned* by removing data points from times of the eclipses¹² and the dips, and also from some other extreme outliers. The cleaned light curve of cycle 462 is shown in the lower panel of Fig. A.1. Such cleaning was performed and two characteristic parameters were extracted interactively for all 35d *Main-On*s observed by ASM and by BAT, the maximum flux and the *turn-on* time. For the maximum flux an interval (of ~3 d) around the maximum was selected and the formal average (and its corresponding uncertainty) of all data points within this interval determined. The turn-on time was found by taking the center between the time of the first significant flux measurement (at the rise from the off-state) and the time of the previous data point. The corresponding uncertainty is half of the difference between those two times.

In addition to the above procedure, a second method was applied for a limited number of 35d cycles, namely a formal best fit to the cleaned light curve using the following function:

$$F(t) = A_0 \times \frac{1}{1 + \exp\left(\frac{A_1 - t}{A_2}\right)} \times \frac{1}{1 + \exp\left(\frac{t - A_3}{A_4}\right)} \quad (\text{A.1})$$

This second method yielded results that were in good agreement with the former procedure. The solid red line in Fig. A.1 is the best fit to the cleaned light curve of 35d cycle 462.

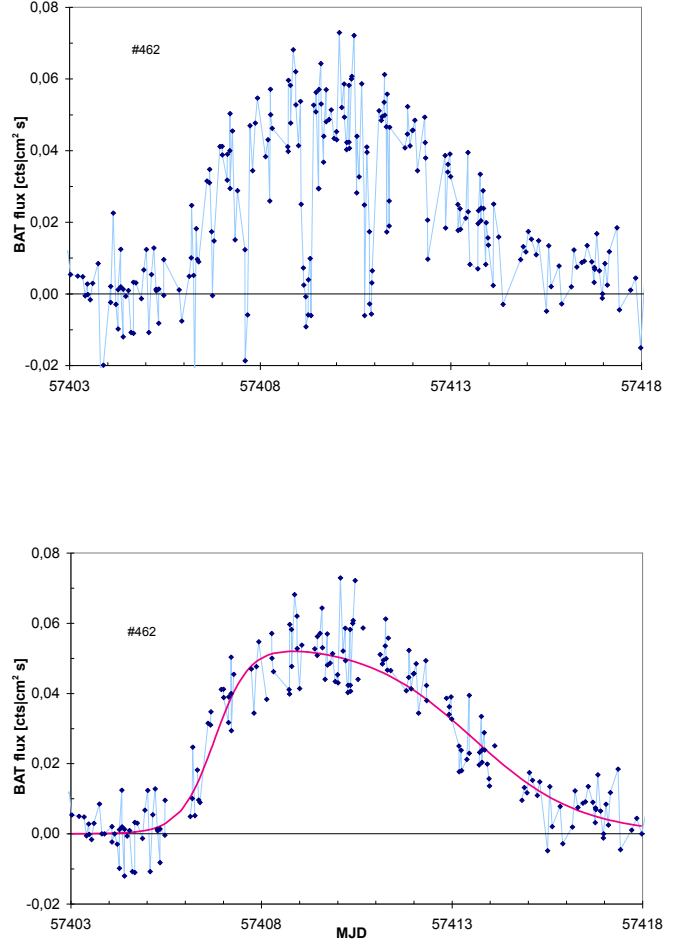


Fig. A.1. Her X-1 light curve for the *Main-On* of 35d cycle 462, representing orbital averages as observed by *Swift*/BAT. Upper panel: observed flux values. Lower panel: *cleaned* data with points during binary eclipses and dips, and extreme outliers, removed. Uncertainties of individual measurements around the maximum flux are of the order of 20%. The solid red line is the best fit function as defined in the text (Eq. A.1). The maximum flux for this 35d cycle is 0.052 ± 0.002 BAT-cts/(cm² s).

A.2. Intercalibration between ASM and BAT

To be able to use flux measurements of the two monitoring instruments *RXTE*/ASM and *Swift*/BAT in a common analysis, an intercalibration was performed. We used the overlapping time period of about 5 yrs (2005–2010) for which both instruments operated simultaneously. Fig. A.2 shows a common light curve of Her X-1 from 1997 to 2016, showing the maximum *Main-On* flux (see previous section). For this light curve the observed BAT maximum values were multiplied with the scaling factor (2–10 keV ASM-cts/s) = $93.0 \times (15\text{--}50\text{ keV BAT-cts cm}^{-2}\text{ s}^{-1})$.

This scaling factor was found by plotting the measured maximum values of both monitors against each other: a linear fit to those values yielded the conversion factor of 93.0 ± 1.3 . As a second method, we used the measured one-day averages from both monitors: the correlation yielded the same result. In order to test, whether the conversion factor showed any time dependence, we divided the overlapping period into five intervals and determined the individual conversion factors. The results are summarized in Table A.1. We conclude that the values are consistent with a con-

¹⁰ <http://xte.mit.edu>

¹¹ <http://swift.gsfc.nasa.gov/results/transients>

¹² For the binary ephemeris of Her X-1 see Staubert et al. 2009.

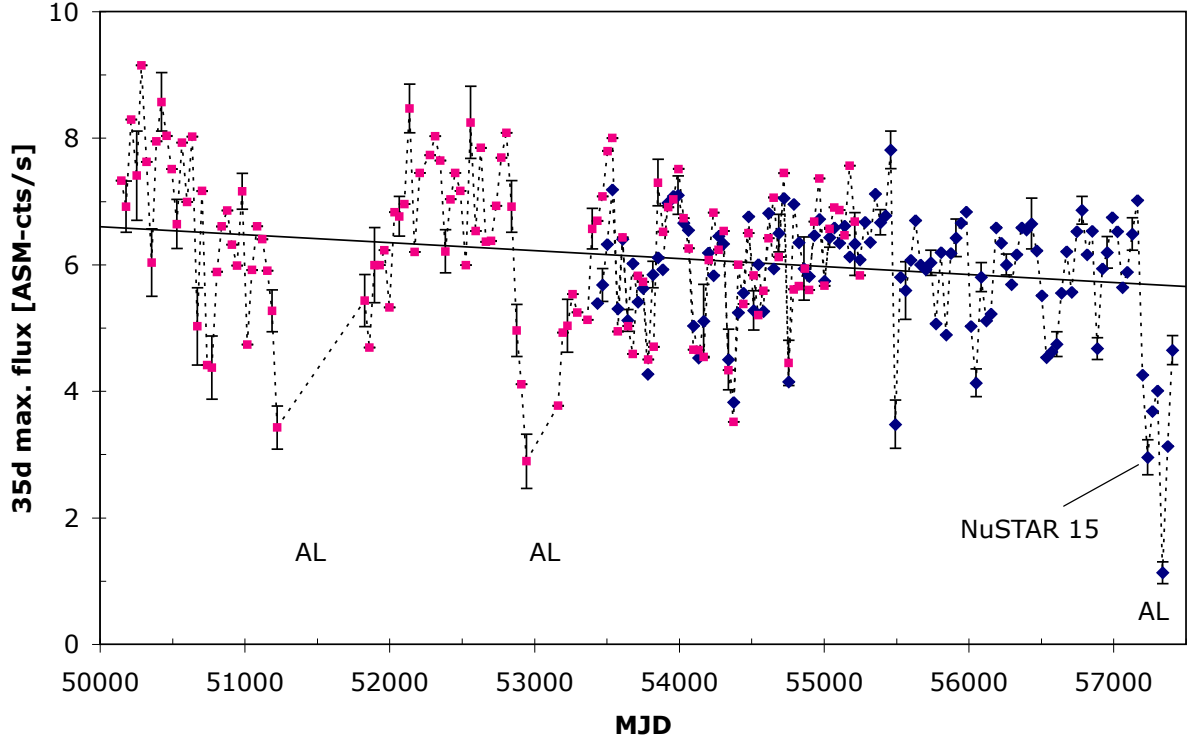


Fig. A.2. Her X-1 long-term light curve, showing the maximum flux of each 35d cycle in units of ASM-cts/s, as determined from observations by the monitoring instruments: red points are from *RXTE*/ASM, blue points are from *Swift*/BAT. Measured BAT values (in units of $\text{cts}/(\text{cm}^2 \text{ s})$) were scaled to ASM-cts/s using the scaling factor determined from the overlapping time period (MJD 53433–55248). For better readability of the light curve, only a few error bars are shown. Three *anomalous lows* (Coburn et al. 2000) can be recognized (indicated by AL). The rather low flux value of the latest *NuSTAR* observation is also marked (NuSTAR 15). The solid line is a linear fit to the data (excluding those points belonging to the ALs). Its slope is $-(1.30 \pm 0.09) 10^{-4}$ (ASM-cts/s)/d, which corresponds to a small reduction in flux of (0.95 ± 0.07) ASM-cts/s over 20 years.

stant conversion factor. When producing frequency distributions of the maximum flux values of Fig. A.2 (over a time period of a few years), we find that they are all consistent with Gaussian distributions with a standard deviation of ~ 1 ASM-cts/s (around 15% of the mean flux). The variation over several 35d cycles, however, can exceed 100%.

Table A.1. Conversion factor f between fluxes measured with ASM and BAT for five shorter time intervals and for the total overlapping time:

$$(2\text{-}10 \text{ keV ASM-cts s}^{-1}) = f \times (15\text{-}50 \text{ keV BAT-cts cm}^{-2} \text{ s}^{-1}).$$

Time interval MJD	f
53430–53800	96.1 ± 3.2
53800–54200	92.8 ± 2.2
54200–54600	90.0 ± 2.5
54600–54950	92.2 ± 3.2
54950–55250	95.5 ± 2.5
total time	
53430–55250	93.0 ± 1.3